Energy Equip. Sys. / Vol. 8/No. 3/Sep. 2020/ 253-262

ENERGY EQUIPSYS

Energy Equipment and Systems

http://energyequipsys.ut.ac.ir
www.energyequipsys.com

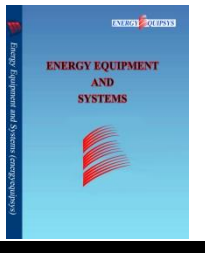

Determination of significant sources generating low-frequency noise in horizontal axis wind turbines

Authors

Alireza Bozorgi [a*]
Ghader Ghorbaniasl [b]

[a] Department of Mechanical Engineering, Arak University of Technology, Arak, Iran

[b] Vrije Universiteit Brussel (VUB), Pleinlaan 2, 1050 Brussels, Belgium

Article history:

Received: 13 August 2020
Accepted : 18 August 2020

ABSTRACT

Several studies show that the Low-Frequency Noise (LFN) of wind turbines could have harmful effects on human health even when it is infrasound. In traditional classifications, the LFN of upwind turbines is referred only to steady thickness and steady loading sources, and the effect of vortices is considered negligible. In this study, the LFN of a horizontal axis wind turbine is simulated in wind speeds of 5-25 m/s by using a hybrid approach. The results show that vortices being far from blades have a significant effect on the LFN. It is also observed that the position received maximum LFN is far from the point introduced by the IEC 61400-11 standard for measuring the noise of horizontal axis wind turbines.

Keywords: Wind Turbine, Noise Pollution, NREL Phase VI, Mean Flow.

1. Introduction

The use of wind turbines known as a reliable solution for decarbonizing electricity generation has increased considerably in recent years, and the increase is expected to accelerate in the near future. The share of wind power in global electricity generation was 5.9% in 2019 [1], and is estimated to reach up to 20% by 2030 [2]. This considerable increase in the share of wind power is possible by developing the use of Horizontal Axis Wind Turbines (HAWTs).

Along with many advantages, wind turbines also have some disadvantages that should be eliminated as much as possible. Noise pollution is the biggest environmental problem of wind turbines that could cause annoyance, sleep disturbance, difficulty concentrating, irritability and fatigue, etc. for people who live near the turbines [4-6]. The range of human hearing is usually defined for frequencies from 20 Hz to 20 kHz, and frequencies below the range are considered infrasound. Because wind turbines rotate slowly, the Low-Frequency Noise (LFN) in the range of infrasound has a significant share in the generated noise. The infrasound has been widely debated as a possible cause of adverse effects of wind turbines on human health, such as dizziness, vertigo, tinnitus, the sensation of aural pain, etc. [7-12]. The study of Hensel et al. [13] shows that the infrasound enters the inner ear and can alter cochlear processing. Moreover, Salt and Hullar [14] concluded that exposure to the infrasound could even affect the physiology of the ear. The results of a functional MRI study done by Dommes et al. [15] also show that the infrasound may activate areas of the primary auditory cortex in the brain. However, there is no regulation about the LFN and infrasound in most

* Corresponding author: Alireza Bozorgi
Department of Mechanical Engineering, Arak University of Technology, Arak, Iran
Email: bozorgi@arakut.ac.ir

countries except Denmark, where the noise of wind turbines in the frequency range of 10-160 Hz must be limited to an A-weighted level of 20 dB [16, 17]. The regulation has been enforced since January 1st 2012.

The aim of this work is to assess the importance of flow-induced sources in LFN generation from the NREL phase VI wind turbine. In addition, a reference position is suggested for measuring the LFN of HAWTs in practical applications. The LFN emitted from the wind turbine is calculated by a hybrid approach, which is widely used in wind turbine problems [18-23]. In this hybrid approach, the flow is simulated with high accuracy in near-field by Computational Fluid Dynamics (CFD) to identify LFN sources, and then, Ffowcs Williams and Hawkings (FW-H) equation [24] is used for the LFN propagation in far-field. In order to include the effect of the mean flow velocity of the radiated noise, the sound field is simulated based on the moving medium solution to the convected FW-H equation derived by Ghorbaniasl and Lacor [27].

Nomenclature

c_0	Speed of sound
f	The function defining the location of data surface
H	Heaviside function
L_i	Dipole type term
n_i	Surface unit normal
p'	Acoustic pressure fluctuation
P_{ij}	Compressive stress tensor
Q	Monopole type term
T_{ij}	Lighthill stress tensor
u_i	Flow velocity
$U_{\infty i}$	Mean flow velocity
v_i	Data surface velocity

Greek letters

δ	Dirac delta function
ρ	Flow density
ρ_0	Undisturbed flow density
σ_{ij}	Viscous stress tensor

Abbreviations

CFD	Computational Fluid Dynamics
LFN	Low-Frequency Noise
OASPL	Overall Sound Pressure Level
RHS	Right Hand Side
SLN	Steady Loading Noise
STN	Steady Thickness Noise

2. Classification of Noise Sources in Wind Turbines

The noise of wind turbines can be divided into mechanical noise, generated from vibration or rubbing of mechanical parts, and into aerodynamic noise generated from airflow passing over blades and other structures. At present, the mechanical noise can be effectively eliminated, but the aerodynamic noise is still the main problem. According to Wagner classification [28], the aerodynamic noise is divided into LFN, inflow turbulence noise and airfoil self-noise (Tabel 1). In this classification, the LFN is due to steady thickness noise (STN) and steady loading noise (SLN), generated only from the rotation of blades, and also due to unsteady loading noise generated from passage of blades through the eddies located around the tower. The latter is only important for downwind configurations (i.e., blades are in the downstream of the tower). Inflow turbulence noise is caused by natural atmospheric turbulence that encounters blades; and airfoil self-noise is due to instabilities in the boundary layer or interaction of boundary layer eddies with blade surface.

3. Flow Simulation

The NREL phase VI turbine is comprised of a two-bladed rotor with a diameter of 10.058 m and a tower with a height of 12.192 m. The blade span, which coincides with the S809 airfoil profile, is twisted and tapered from the root to the tip.

Flow simulation can be performed by using the steady RANS equations in a rotating frame for defining steady noise sources. The flow simulation has been performed before by the authors [25] for the turbine in upwind configuration (blades are located in the upstream of the tower), with the pitch angle of 3o and the cone angle of 0o. The configuration and the operational conditions were according to the sequence S of experimental tests performed by Hand et al. [26].

Table1. Aerodynamic noise sources in HAWTs [28]

Type or indication	Mechanism
Low-frequency noise	
Steady thickness noise	Rotation of blades
Steady loading noise	Rotation of blades
Unsteady loading noise	Passage of blades through tower velocity deficit or wakes (important for downwind turbines)
Inflow turbulence noise	Interaction of blades with atmospheric turbulence
Airfoil self-noise	
Trailing-edge noise	Interaction of boundary layer turbulence with blade trailing edge
Tip noise	Interaction of tip turbulence with blade tip surface
Stall, separation noise	Interaction of turbulence with blade surface
Laminar boundary layer noise	Non-linear boundary layer instabilities interacting with the blade surface
Blunt trailing edge noise	Vortex shedding at the blunt trailing edge
Noise from flow over holes, slits and intrusions	Unstable shear flows over holes and slits, vortex shedding from intrusions

In the simulation [25], the tower was ignored since its effect is negligible on the performance of upwind turbines. Moreover, the flow domain was defined around only one blade with considering the rotational periodic boundary condition (Fig. 1). After a mesh independence study, a fine mesh with about 3.6e+6 cells was selected for all simulations. Then, the continuity and steady RANS equations coupled with the Shear-Stress Transport (SST) turbulence model were solved in Ansys CFX 16. The simulation continued until fluctuations on the calculation of the thrust and power reached to less than 0.05% for more than 500 iterations.

As shown in Fig. 2, the numerical results obtained by the authors [25] are in good agreement with the experiment [26], in comparison with other numerical studies [29, 30]. In [25], the simulation has been performed for wind speeds of 5-25 m/s, the rotational speed of N = 72 rpm and the air density of ρ = 1.225 kg/m^3. Then, the LFN was calculated with considering only STN and SLN sources, being on the blade's surface. However, in the present work, the results of the flow simulation are used for defining all steady noise sources; and in addition to STN and SLN sources, the sources related to vortices are also calculated. Moreover, the aeroacoustic solver must be developed to have the capability of calculating the noise of new sources.

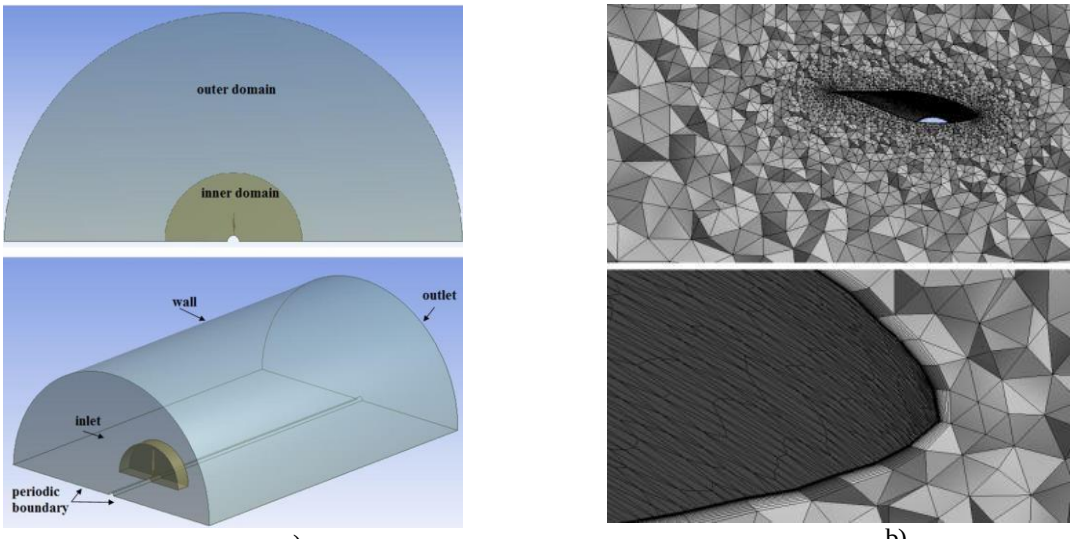

a) b)

Fig. 1: a) Computational domain and boundary conditions
b) Mesh and boundary layer grids around the blade [25]

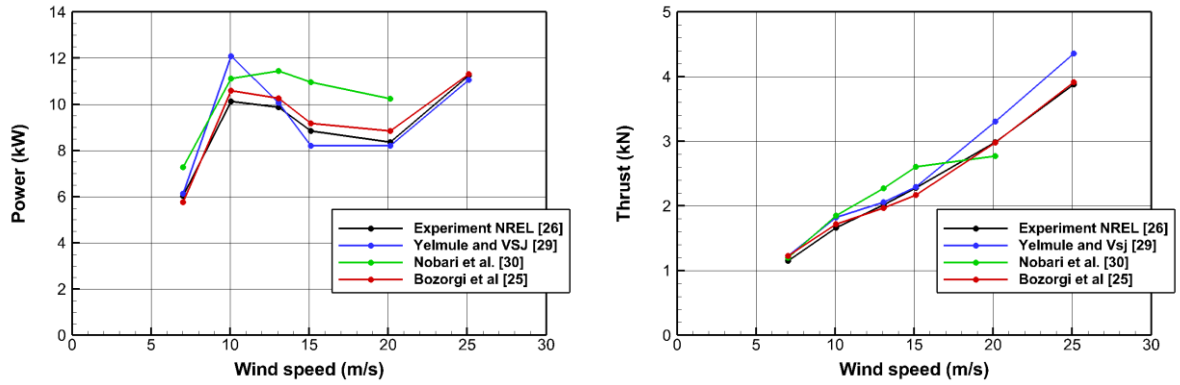

a) b)

Fig. 2. Comparison of the CFD and Experimental data for a) power, b) thrust [25]

4. Far-field noise propagation

The FW-H equation [24] is an exact rearrangement of the continuity and Navier-Stokes equations and is widely used for calculating the noise of moving bodies. A generalized form of this equation [27] is applied for far-field LFN calculation, including the effect of mean flow velocity U_∞ on the noise propagation as follows:

$$\left\{\frac{1}{c_0^2}\frac{\mathrm{D}^2}{\mathrm{D}t^2}-\frac{\partial^2}{\partial x_i^2}\right\}\left[p'(\mathbf{x},t)H(f)\right]=\frac{\partial}{\partial t}\left[Q\delta(f)\right]-\frac{\partial}{\partial x_i}\left[L_i\delta(f)\right]+\frac{\partial^2}{\partial x_i\partial x_j}\left[T_{ij}H(f)\right] \quad (1)$$

where,

$$\frac{\mathrm{D}}{\mathrm{D}t}=\frac{\partial}{\partial t}+U_{\infty i}\frac{\partial}{\partial x_i} \quad (2)$$

In Eq. (1), c_0 is the speed of sound, p′ is pressure fluctuations, H is the Heaviside function, and δ is the Dirac delta function. Moreover, $f(x.t)=0$ defines the position of DS enclosing the body, such that we have inside of DS $f(x.t)<0$ and outside of it $f(x.t)>0$. In RHS of Eq. (1), the terms of Q, Li and Tij represent monopole type source, dipole type source and quadrupole source, respectively. Using the properties of the Dirac delta function, Q and Li are needed to calculate only on DS ($f(x.t)=0$), and are given by

$$Q=\rho\left(u_j-v_j\right)n_j+\rho_0 v_j n_j \quad (3)$$

$$L_i=\rho\left(u_i-U_{\infty i}\right)\left(u_j-v_j\right)n_j+P_{ij}n_j$$

The T_{ij} term must be calculated for $f(x.t)>0$ given by

$$T_{ij}=\rho\left(u_i-U_{\infty i}\right)\left(u_j-U_{\infty j}\right)+\left[\left(p-p_0\right)-c_0^2\left(\rho-\rho_0\right)\right]\delta_{ij}-\sigma_{ij} \quad (4)$$

Here, ρ is the density, ρ_0 is the undisturbed density, uj and vj denote the j-th component of flow velocity and DS velocity, respectively, and nj represents the j-th component of unit normal vector at DS. Moreover, Pij is the compressive stress tensor, and σij is the viscous stress tensor.

In the original FW-H equation, DS is coincident with the body surface and is impermeable, but it can be defined far from the body and thus be permeable. The Q and Li terms are equal to the thickness and loading sources, respectively, where DS is coincident with the body surface. However, when DS is defined far from the body, the Q and Li terms, in addition to thickness and loading sources, include the quadrupole sources (Tij term) that are located inside of DS [31]. The Tij term represents the effect of wakes and vortices on noise generation [32, 33].

In the present work, permeable DSs are used for the surface noise sources, where the effect of vortices on LFN can be included. The solver has been developed based on the well-known moving medium formulation of Ghorbaniasl and Lacor [27].

5. Results

According to the IEC 61400-11 standard, which is used for noise measurement of HAWTs, microphone position is in downstream with

$$R_H=H+D/2;\ R_V=H \quad (5)$$

where R_H and R_v are horizontal and vertical distances from the rotor center, respectively, D is turbine diameter, and H is hub height from the ground. By using Eq. (5), the

microphone must be located at $R = 21$m and θ = -55° for the NREL phase VI turbine (R and θ are defined in Fig. 3). Here, the LFN is calculated in this position and also in several other positions with R = 21 m and $-75^o \le \theta \le 75^o$. Outside of the θ range, the LFN is very weak, such that the Overall Sound Pressure Level (OASPL) goes to −∞ dB at θ = -90° and 90° (on rotation axis). It can be shown by the formulation 1A [27] that LFN is generated by steady noise sources only if observer-source distance changes when blades rotate. However, on the rotation axis, the distance is unchanged when blades rotate, and the LFN is zero (−∞ in the logarithmic scale) on the axis.

It is expected that with moving away from blades since vortices are dissipated, and flow tends to be uniform, the effect of vortices on the LFN decreases. The question is how far from blades vortices have no significant effect on LFN. For answers to this question, several DSs are defined around the blade by scaling the blade span (Fig. 4) with a scale factor of 1 to 15; and a convergence criterion is defined for finding final DS surrounding all important LFN sources. The criterion is that the difference between the LFN calculated from two consecutive DSs reaches to less than 0.5 dB in all observer positions. The results in Fig. 5 show that the final DS at wind speeds of 5 and 10 m/s is DS 5, at a wind speed of 15 m/s is DS 13, and at wind speeds of 20 and 25 m/s is DS 15 (the DS number is equal to scale factor).

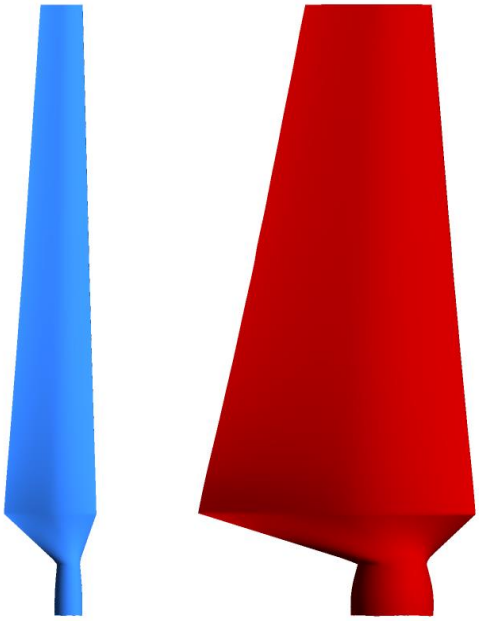

Fig. 4. Blade surface (blue) and a permeable data surface (red) surrounding the blade

The results of the final DSs show that the maximum LFN is in downstream. This maximum is at θ = -30° for all wind speeds, except U_∞=10 m/s, that the maximum is located at θ = -15°. However, for U_∞=10 m/s, the difference between the noises at $\theta = -15^o$ and -30° is less than 0.2 dB, which is ignorable and also is less than the convergence criterion (0.5 dB). Therefore, the point with R = 21m and θ = -30° can be defined as a reference position for measuring the LFN of the HAWT

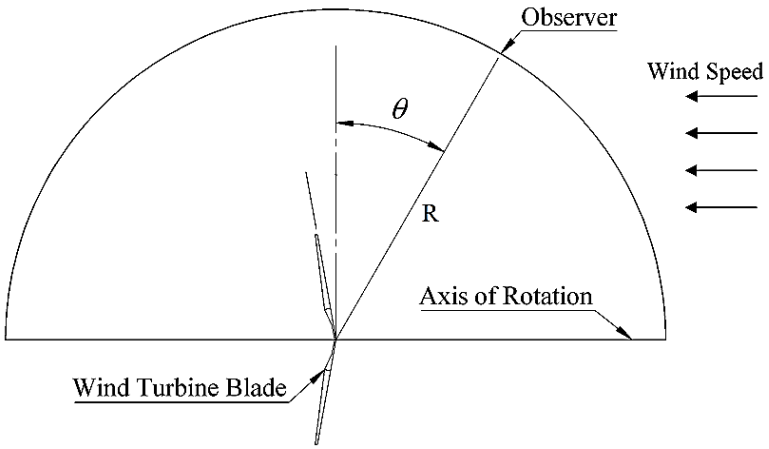

Fig. 3. The description of the observer position [25]

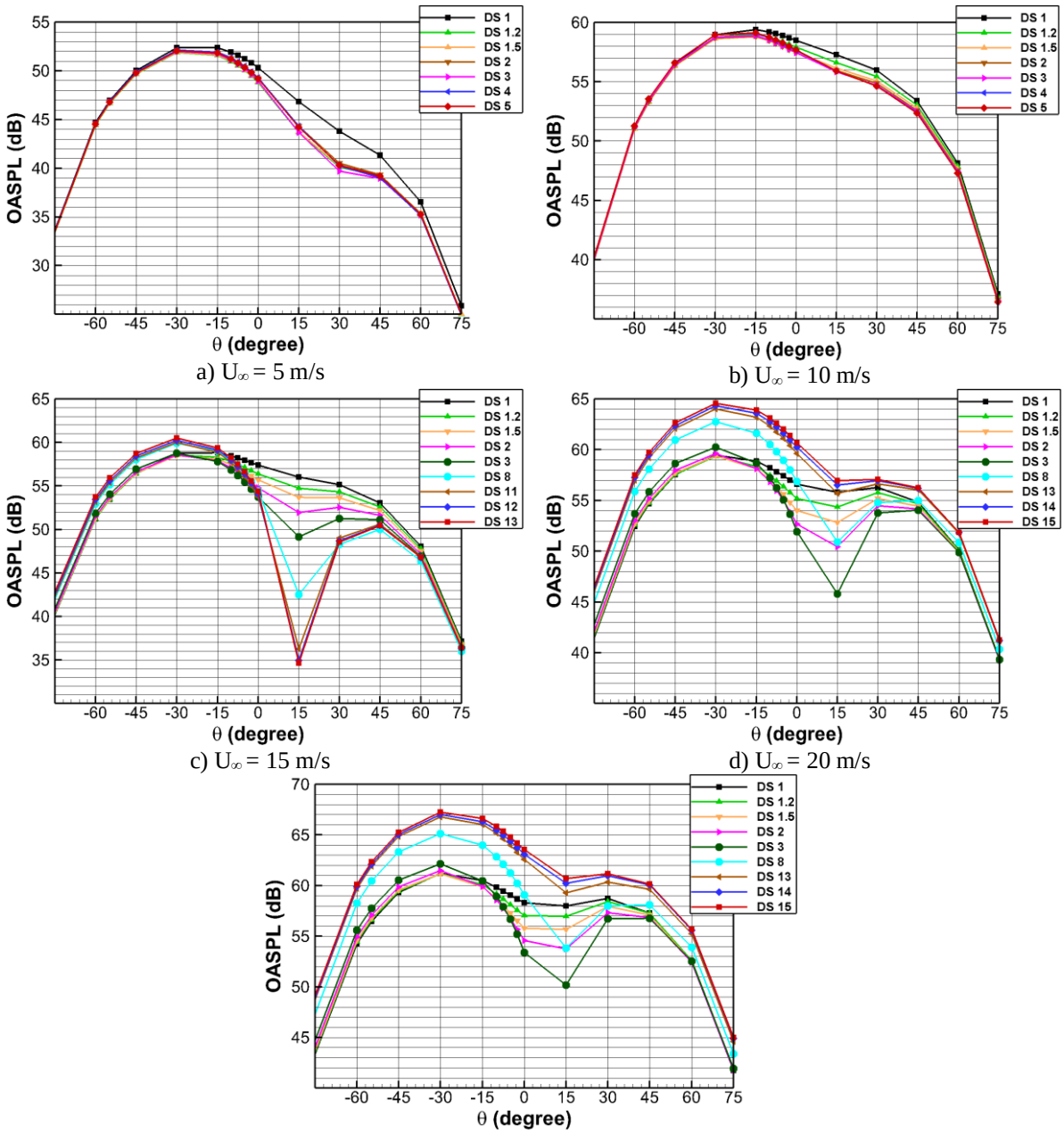

a) U_∞ = 5 m/s

b) U_∞ = 10 m/s

c) U_∞ = 15 m/s

d) U_∞ = 20 m/s

e) U_∞ = 25 m/s

Fig.5. LFN calculation using different DSs

in wind speeds of 5-25 m/s. The reference position is far from the microphone position, where the IEC 61400-11 standard introduces for measuring the noise of HAWTs (R = 21m and θ = -55°). Therefore, it seems that the microphone position is not appropriate for the evaluation of LFN. However, further studies are needed for a definite conclusion. For example, different test cases should be investigated; moreover, the effect of ground, tower of turbines, etc. on the LFN must also be considered.

For a more detailed investigation, the directivity pattern of Q and L_i terms are separately shown in Fig. 6. Here, the results obtained by using the DS 1 (containing only STN and SLN sources) and the final DSs (containing all significant steady sources) are compared with each other. The comparison of the Q term between DS 1 and final DS shows that the steady noise sources being off the blades (vortices) have a considerable effect on the directivity. It is observed that the sources weaken the noise generated by the Q term at the wind speed of 5 m/s (Fig. 6a),

while they amplify it in higher wind speeds (Fig. 6b-6e). The comparison of the L_i term between DS 1 and final DS also shows that vortices have a considerable effect on the noise of the L_i term. The effect of them in decreasing or increasing the noise of L_i term is dependent on observer position.

With considering the results of final DSs, it is observed that in low wind speeds (U_∞ = 5 and 10 m/s) the noise of Q term is less than Li term, but in high wind speeds (U_∞ = 5 and 10 m/s) the noise of Q term is more. In other words, the Q term is more amplified by increasing wind speed.

In addition to the magnitude of the noise of Q and L_i terms, the phase difference between the noises can be a significant effect on the LFN. For example, the time history of the noises at U_∞ = 25 m/s is shown in Fig. 7. It is observed that the phase difference is such

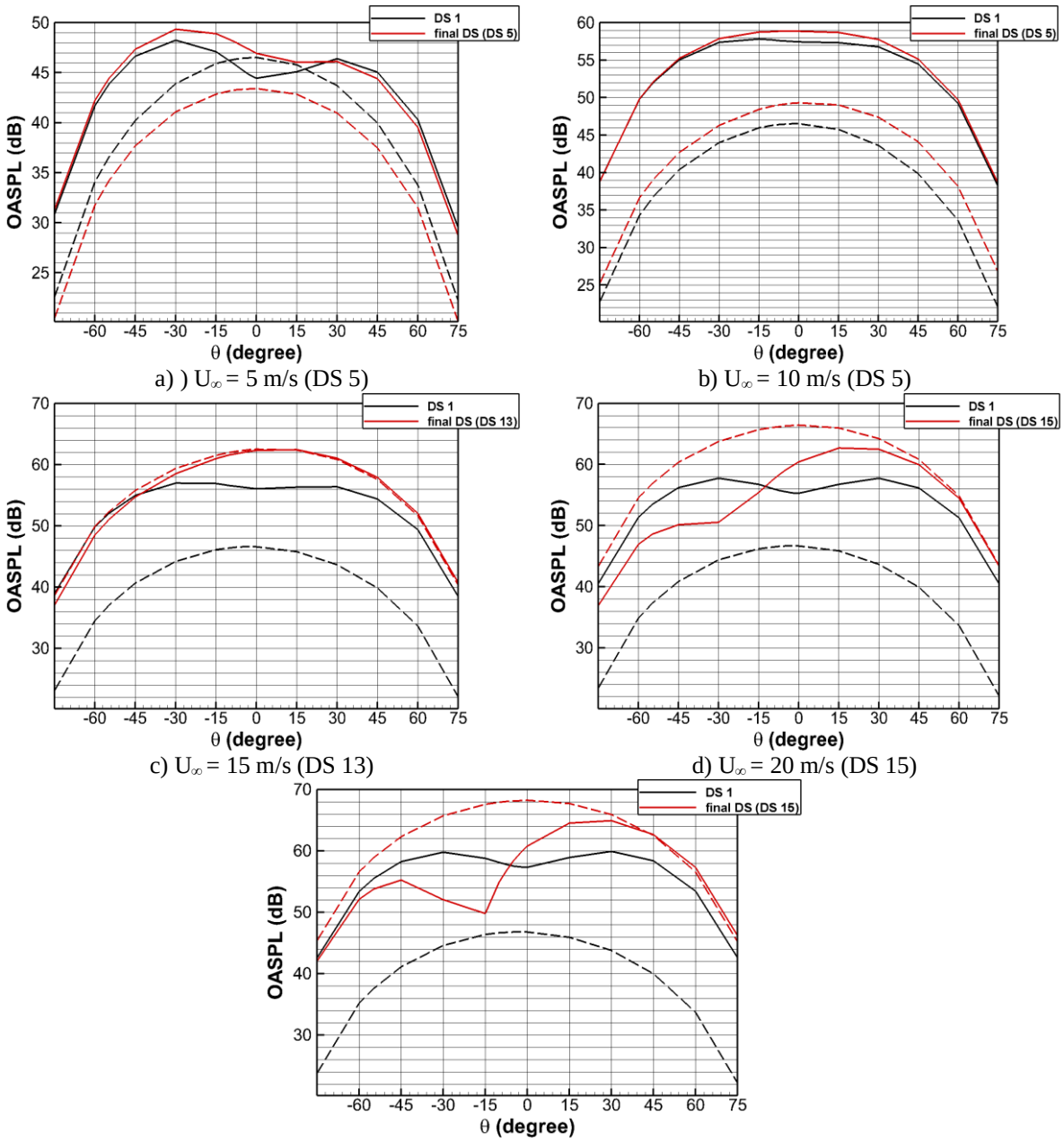

a)) U_∞ = 5 m/s (DS 5)

b) U_∞ = 10 m/s (DS 5)

c) U_∞ = 15 m/s (DS 13)

d) U_∞ = 20 m/s (DS 15)

e) U_∞ = 25 m/s (DS 15)

Fig.6. The effect of DS on the directivity of Q (------) and L_i (——)

that the noises weaken each other in $\theta \geq -15^{o}$, while they amplify each other in $\theta < -15^{o}$. Therefore, although Q and L_i noises in downstream are less than upstream or are equal (Fig. 6e), because of phase difference effect, LFN in downstream is more than upstream (Fig 5e).

It should be mentioned that, although the blades rotate with a constant speed, Q and L_i noises are not fully sinusoidal since the distance between the observers and the LFN sources is not a sinusoidal time function. For example, the results for $\theta = -15^{o}$ (Fig. 7g) show that the deviation from the sinusoidal function is very high for the L_i noise.

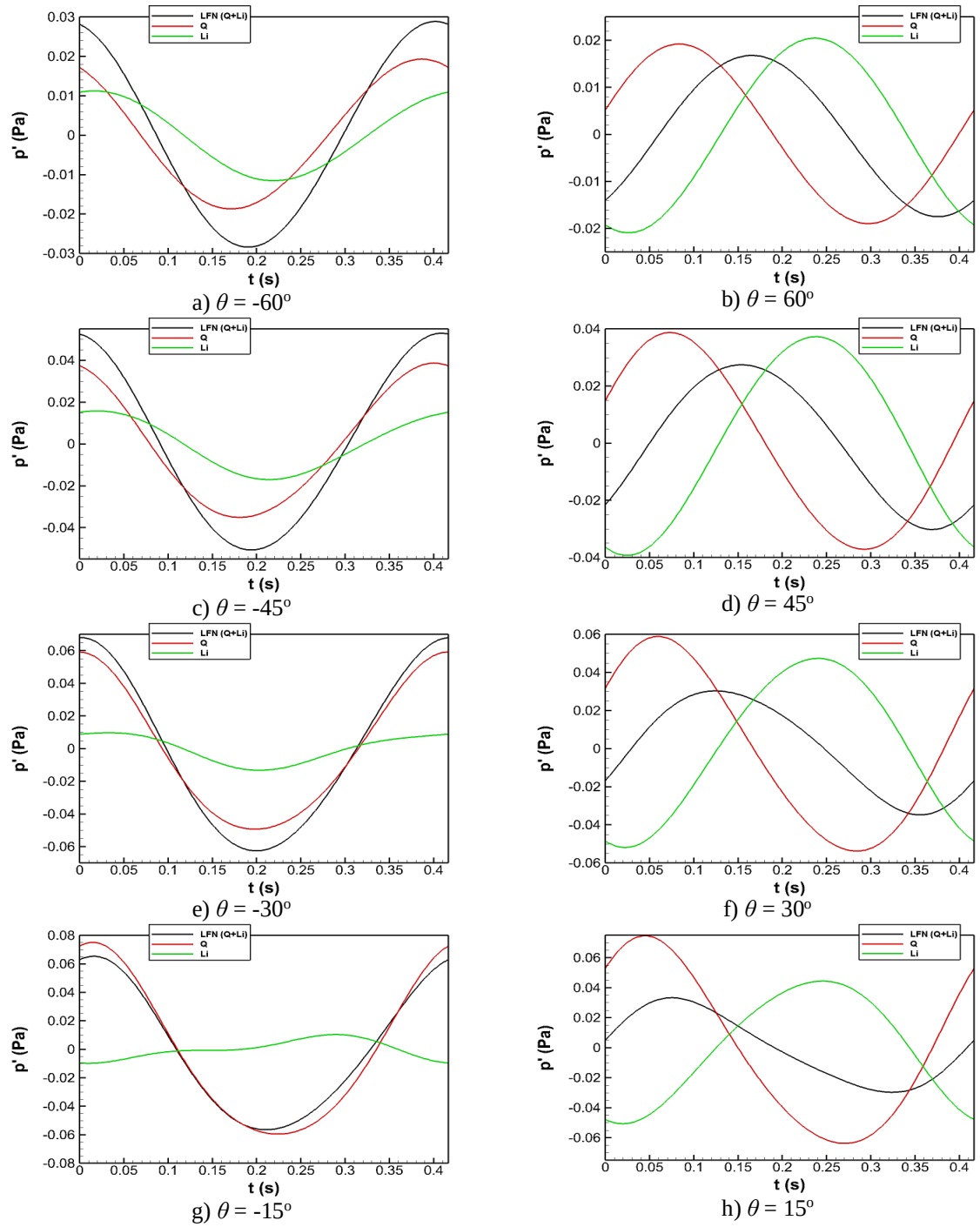

a) θ = -60° b) θ = 60°

c) θ = -45° d) θ = 45°

e) θ = -30° f) θ = 30°

g) θ = -15° h) θ = 15°

Fig.7. Time history of LFN for U_{∞} = 25 m/s in different observer positions

6. Conclusion

In the present work, LFN generated by a small wind turbine (NREL phase VI) was investigated by a hybrid approach. In this approach, first, flow is simulated by CFD for defining LFN sources on a DS, and then, the noise propagated from the DS is calculated by the solution for the convected FW-H equation. Here, the wind speed was considered in the range of 5-25 m/s, and the LFN was calculated in different observer positions with $R = 21$ m and $-75^o \le \theta \le 75^o$.

In traditional classifications, only the STN and SLN sources (defined on blades surface) have been known as the main sources of LFN generation in upwind turbines. However, the results of the present work showed that in addition to the STN and SLN sources, vortices being off the blades significantly participate in the LFN generation. Moreover, the results show that the Q term is more amplified by increasing wind speed, in comparison with the L_i term.

It was concluded that the point with R = 21 m and θ = –30° could be defined as a reference position for measuring the maximum LFN of the wind turbine in wind speeds of 5-25 m/s. However, the reference position is far from where the IEC 61400-11 standard introduces for measuring the noise of HAWTs (R = 21 m and $\theta = -55^o$). Therefore, it is suggested that a separate position should be introduced by the standard for measuring LFN. However, further studies with several test cases and parameter studies such as ground surface and the tower turbine should be performed to draw a definite conclusion.

References

[1] REN21, R., Renewable 2020 Global Status Report, REN21 Secretariat, Paris, France. 2020, ISBN 978-3-948393-00-7.

[2] Fried, L., et al., Global Wind Outlook 2016. 2016.

[3] Tummala, A., et al., A review on small scale wind turbines. Renewable and Sustainable Energy Reviews, 2016. 56: p. 1351-1371.

[4] Bakker, R.H., et al., Impact of wind turbine sound on Annoyance, self-reported sleep disturbance and psychological distress. Science of The Total Environment, 2012. 425: p. 42-51.

[5] Van Renterghem, T., et al., Annoyance, detection and recognition of wind turbine noise. Science of the Total Environment, 2013. 456: p. 333-345.

[6] Waye, K.P. and E. ÖHrstrÖM, PSYCHO-ACOUSTIC CHARACTERS OF RELEVANCE FOR ANNOYANCE OF WIND TURBINE NOISE. Journal of Sound and Vibration, 2002. 250(1): p. 65-73.

[7] Harry, A., Wind turbines, noise and health. Available from: http: i'/www. f| atgroup. co. uk/pdf/wtnoise_health__2007_a_barry. pdf, 2007.

[8] Pierpont, N., Wind turbine syndrome: A report on a natural experiment. 2009: K-Selected Books Santa Fe, NM.

[9] Shepherd, D., et al., Evaluating the impact of wind turbine noise on health-related quality of life. Noise and Health, 2011. 13(54): p. 333.

[10] Nissenbaum, M.A., J.J. Aramini, and C.D. Hanning, Effects of industrial wind turbine noise on sleep and health. Noise and Health, 2012. 14(60): p. 237.

[11] Inagaki, T., Y. Li, and Y. Nishi, Analysis of aerodynamic sound noise generated by a large-scaled wind turbine and its physiological evaluation. International Journal of Environmental Science and Technology, 2015. 12(6): p. 1933-1944.

[12] Swinbanks, M. Direct Experience of Low Frequency Noise and Infrasound within a Windfarm Community. in 6th International Meeting on Wind Turbine Noise, Glasgow. 2015.

[13] Hensel, J., et al., Impact of infrasound on the human cochlea. Hearing research, 2007. 233(1): p. 67-76.

[14] Salt, A.N. and T.E. Hullar, Responses of the ear to low frequency sounds, infrasound and wind turbines. Hearing research, 2010. 268(1): p. 12-21.

[15] Dommes, E., et al., Auditory cortex stimulation by low-frequency tones—An fMRI study. Brain Research, 2009. 1304: p. 129-137.

[16] Jakobsen, J., Danish regulation of low frequency noise from wind turbines. Journal of low frequency noise, vibration and active control, 2012. 31(4): p. 239-246.

[17] Schmidt, J.H. and M. Klokker, Health effects related to wind turbine noise exposure: a systematic review. PLoS One, 2014. 9(12): p. e114183.
[18] Tadamasa, A. and M. Zangeneh, Numerical prediction of wind turbine noise. Renewable energy, 2011. 36(7): p. 1902-1912.
[19] Ghasemian, M. and A. Nejat, Aerodynamic noise prediction of a horizontal Axis wind turbine using improved delayed detached eddy simulation and acoustic analogy. Energy Conversion and Management, 2015. 99: p. 210-220.
[20] Luo, K., et al., Large-eddy simulation and wind-tunnel measurement of aerodynamics and aeroacoustics of a horizontal-axis wind turbine. Renewable Energy, 2015. 77: p. 351-362.
[21] Ma, P., F.-S. Lien, and E. Yee, Coarse-resolution numerical prediction of small wind turbine noise with validation against field measurements. Renewable Energy, 2017. 102: p. 502-515.
[22] Maizi, M., et al., Noise reduction of a horizontal wind turbine using different blade shapes. Renewable Energy, 2018. 117: p. 242-256.
[23] Zhang, S., et al., Influences of operating parameters on the aerodynamics and aeroacoustics of a horizontal-axis wind turbine. Energy, 2018. 160: p. 597-611.
[24] Williams, J.F. and D.L. Hawkings, Sound generation by turbulence and surfaces in arbitrary motion. Philosophical Transactions of the Royal Society of London. Series A, Mathematical and Physical Sciences, 1969. 264(1151): p. 321-342.
[25] Bozorgi, A., G. Ghorbaniasl, and S. Nourbakhsh, the reduction in low-frequency noise of horizontal-axis wind turbines by adjusting blade cone angle. International Journal of Environmental Science and Technology, 2018: p. 1-14.
[26] Hand, M., et al., Unsteady aerodynamics experiment phase VI: wind tunnel test configurations and available data campaigns. National Renewable Energy Laboratory, Golden, CO, Report No. NREL/TP-500-29955, 2001.
[27] Ghorbaniasl, G. and C. Lacor, A moving medium formulation for prediction of propeller noise at incidence. Journal of Sound and Vibration, 2012. 331(1): p. 117-137.
[28] Wagner, S., R. Bareiss, and G. Guidati, Wind turbine noise. 2012: Springer Science & Business Media.
[29] Yelmule, M.M. and E.A. Vsj, CFD predictions of NREL phase VI rotor experiments in NASA/AMES wind tunnel. International Journal of Renewable Energy Research (IJRER), 2013. 3(2): p. 261-269.
[30] Nobari, M., E. Mirzaee, and M. Nosratollahi, Improvement of wind turbine performance using a novel tip plate structure. Energy Conversion and Management, 2016. 123: p. 592-609.
[31] Di Francescantonio, P., A new boundary integral formulation for the prediction of sound radiation. Journal of Sound and Vibration, 1997. 202(4): p. 491-509.
[32] Farassat, F. Quadrupole source in prediction of the noise of rotating blades-A new source description. in American Institute of Aeronautics and Astronautics Conference. 1987.
[33] Farassat, F. and B. Kenneth S, The uses and abuses of the acoustic analogy in helicopter rotor noise prediction. 1987.